REPORTS IN METEOROLOGY AND OCEANOGRAPHY
UNIVERSITY OF BERGEN 1 - 2007

CURRENT MEASUREMENTS AT THE STORFJORDEN SILL: SEPTEMBER 2004 – AUGUST 2006

ILKER FER

Geophysical Institute, University of Bergen

November, 2007

UNIVERSITETET I BERGEN

Geophysical Institute
University of Bergen
Bergen, Norway

«REPORTS IN METEOROLOGY AND OCEANOGRAPHY»

utgis av Geofysisk Institutt ved Universitetet I Bergen.

Formålet med rapportserien er å publisere arbeider av personer som er tilknyttet avdelingen.

Redaksjonsutvalg:

Peter M. Haugan, Frank Cleveland, Arvid Skartveit og Endre Skaar.

Redaksjonens adresse er : «Reports in Meteorology and Oceanography»,

Geophysical Institute.

Allégaten 70

N-5007 Bergen, Norway

RAPPORT NR: 1 - 2007

ISSN 1502-5519

ISBN 82-8116-012-8

Contents

1. Introduction

Under the EU project "Developing Arctic Modelling and Observing Capabilities for Long-term Environment Studies- DAMOCLES", Geophysical Institute/University of Bergen is maintaining an acoustic Doppler current profiler (ADCP) at the sill separating the Storfjorden in Svalbard Archipelago and Storfjordrenna north of Storfjordbanken on the Barents Sea shelf (Figure 1). Storfjorden, through its polynya activity, produces highly saline water near the freezing temperature which fills the fjord to the sill level (115 m) and initiates a gravity driven overflow [*Quadfasel et al.*, 1988; *Schauer*, 1995; *Schauer and Fahrbach*, 1999; *Fer et al.*, 2003; *Fer et al.*, 2004; *Skogseth et al.*, 2005a]. The overflow water is dense enough to penetrate below the Atlantic Water at the region. Because Storfjorden-origin water is occasionally observed in the deep Fram Strait [*Quadfasel et al.*, 1988], it is considered to contribute to the ventilation of the Arctic Ocean. The objective of the deployment is to monitor the overflow, its (estimate of) volume flux, its interannual variability (through scheduled deployments every year) as well as high and low frequency variability at the sill.

A detailed report for the first year of the measurements (2004) was published in Geophysical Institute's report series [*Fer*, 2006] including processing details, data quality and observed velocity statistics, inferred tides and frequency domain descriptions derived from the data. Here we report on the data acquired for three years from 2004 to 2006, with focus on interannual comparison.

2. The instrumentation, deployment and recovery

A self-contained 307.2 KHz broadband Workhorse, Sentinel, RD Instruments ADCP was deployed at the Storfjorden sill (Figure 1, Table 1) to record for the duration of freezing and overflow period in 2004 to 2006. The instrument is installed in an aluminium trawl-proof frame, attached to a concrete block of 2.5x2.5x0.37 m dimensions. The weight of the concrete block is about 2.5 (1.6) tones in air (water). The frame with instruments (acoustic release, ADCP and the battery pack) and flotation elements installed is 300 kg in air. Overall height of the installation is 86 cm.

Table 1. Deployment Summary

Year	Longitude	Latitude	Depth (m)	Deployed (UTC)	Retrieved (UTC)	Recovered Data Length (Day)
2004	019° 15′E	76° 58′ N	111	04092003 1730	19082004 1300	349.71
2005	019° 15′E	76° 58′ N	111	17122004 1915	12082005 0622	236.96
2006	019º 14.95′ E	76º 58.08′N	114	12122005 1431	09082006 1520	239.96

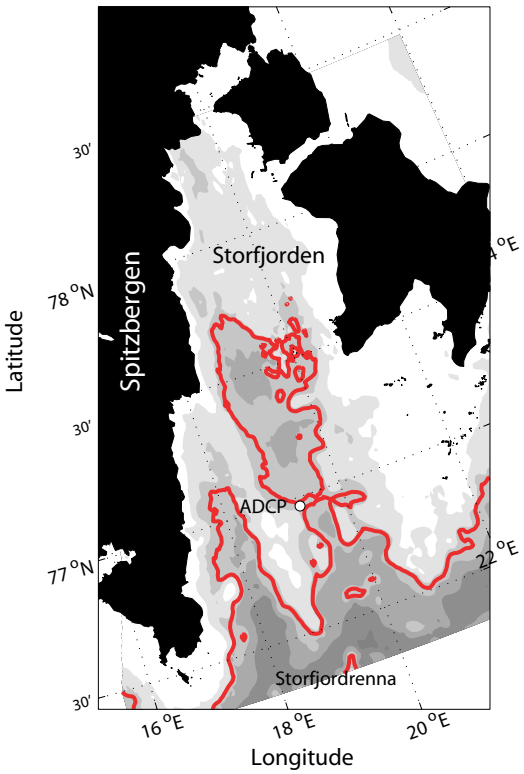

Figure 1. Map of the region. Isobaths, shaded at 50-m intervals, are derived from the recent high-resolution bathymetry [*Skogseth et al.*, 2005b]. Red isobath (= 120 m) is shown to identify the sill. ADCP position is marked by the circle.

Figure 2. (left) The trawl-proof frame during deployment in summer 2003. (above) A close-up of the instruments before the 2006 deployment. The ADCP transducers are covered by the yellow protective cap removed before the deployment. The blue case on the left is the external battery unit. Horizontally installed is the Sea-Bird Microcat SBE37SM. (Pictures by F. Cleveland.)

The configuration of the ADCP is detailed in Appendix A. Four beams (transducers) are slanted at 20° from horizontal, in Janus configuration. In all deployments ADCP sampled at 4-m depth cell size (bins hereafter) averaging data (33 pings per ensemble) at 10 min intervals. The first bin was centered at about 6 mab (meter above bottom). The data are

recorded in Earth co-ordinates. In addition to profiling the horizontal and vertical velocity components, ADCP is equipped with temperature (mounted on transducer, precision ± 0.4°C, resolution 10 mK), tilt (accuracy ±0.5°, resolution 0.01°) and compass (accuracy ± 2°, resolution 0.01°) sensors. When sampled at 4-m bins the ADCP has a typical range of 86-113 m with a single ping standard deviation of 3 cm s^{-1}. Because random error is uncorrelated from ping to ping, averaging reduces the standard deviation of the velocity error by the square root of the number of pings [*RDI*, 1996], in our case by a factor $(33)^{-1/2} = 0.174$, yielding 0.5 cm s^{-1}.

In 2006 the frame was equipped with a Sea-Bird SBE37SM Microcat (S/N 4011), temperature-conductivity-pressure recording unit. The Microcat was not equipped with an internal pump. It acquired one sample every 10 minutes (i.e., no averaging was done before recording).

3. ADCP Data processing

Data are flagged when the percent good of 3 and 4 beam solutions are less than 70 or the magnitude of the error velocity[1] is greater than 5 cm s^{-1} or any of the velocity components exceeded 10 m s^{-1}. Flagged data are treated as missing values and portions with gaps less than 1 hour duration (6 ensembles) are interpolated. Larger portions remain as gaps in the data.

Spikes in velocity components and temperature data are detected and removed in two runs. In the first (second) run, points exceeding 2.5 (3) times the standard deviation of de-meaned data at 40 scan moving windows are detected, removed, and interpolated. The difference between the original data and de-spiked data is calculated. In each run, the original data are retained when the magnitude of this difference was less than twice its rms value over the whole record.

The sound speed used by the ADCP, C_{ADCP}, was set for S = 35 and T = 5°C at 115 dbar pressure. Assuming constant S = 35 and using the bottom temperature measured by the ADCP we calculate the sound speed, C_{real}, and correct the horizontal velocity components by a factor C_{real}/C_{ADCP} for each ensemble [*RDI*, 1996]. The sound speed is not sensitive to salinity and S = 35 is adequate for the site.

The surface is detected as the bin with the maximum echo intensity[2]. The strong echo from the surface (or from ice when present) can overwhelm the side lobe suppression of the transducer. For 20° beam angle the last 6% of the range to the surface is contaminated and is removed from the data. In practice we report on only the first 23 bins, i.e. 94 mab, which excludes the last 15% of the water depth of 111 m. The horizontal velocity components are rotated to account for the magnetic declination. At the mooring location the rate of change of the magnetic declination is negligible throughout the annual sampling period. Therefore the value at the mid-time of each experiment is used: 26022004 UTC, +6° 51′E; 15042005 UTC +7° 9′E; 11042006 UTC +7° 35′E, respectively.

4. ADCP Data quality

Monthly average vertical profiles of parameters describing the data quality are shown in Figure 3. Data quality statistics for each bin are tabulated for each year in Table 2. The average correlation over 4 beams, the percent good of 3 or 4 beam solutions, the echo

[1] The fourth beam of the ADCP provides for a redundant estimate of the vertical velocity. The error velocity is the difference between the two estimates of vertical velocity. It allows us to evaluate whether the assumption of horizontal homogeneity, within the depth bin, is reasonable.

[2] Echo intensity is the signal strength of the echo returning from the ADCP's transmit pulse

intensity and rms error velocity are shown after excluding the flagged (bad) data. In the lower 50 m, the data quality is very good with echo intensity between 79-129 counts, on the average, and only <1% of the data from each bin is flagged. Between 50-66 m typically within 10% of the data is excluded. At bins above 70 mab standard deviation of the error velocity is about 1-3 cm s^{-1} and echo intensity is significantly reduced. There is seasonal variation on the achieved vertical range of good data, suggesting less scatterer in the water column between February and May. Data quality is comparable for all three deployments.

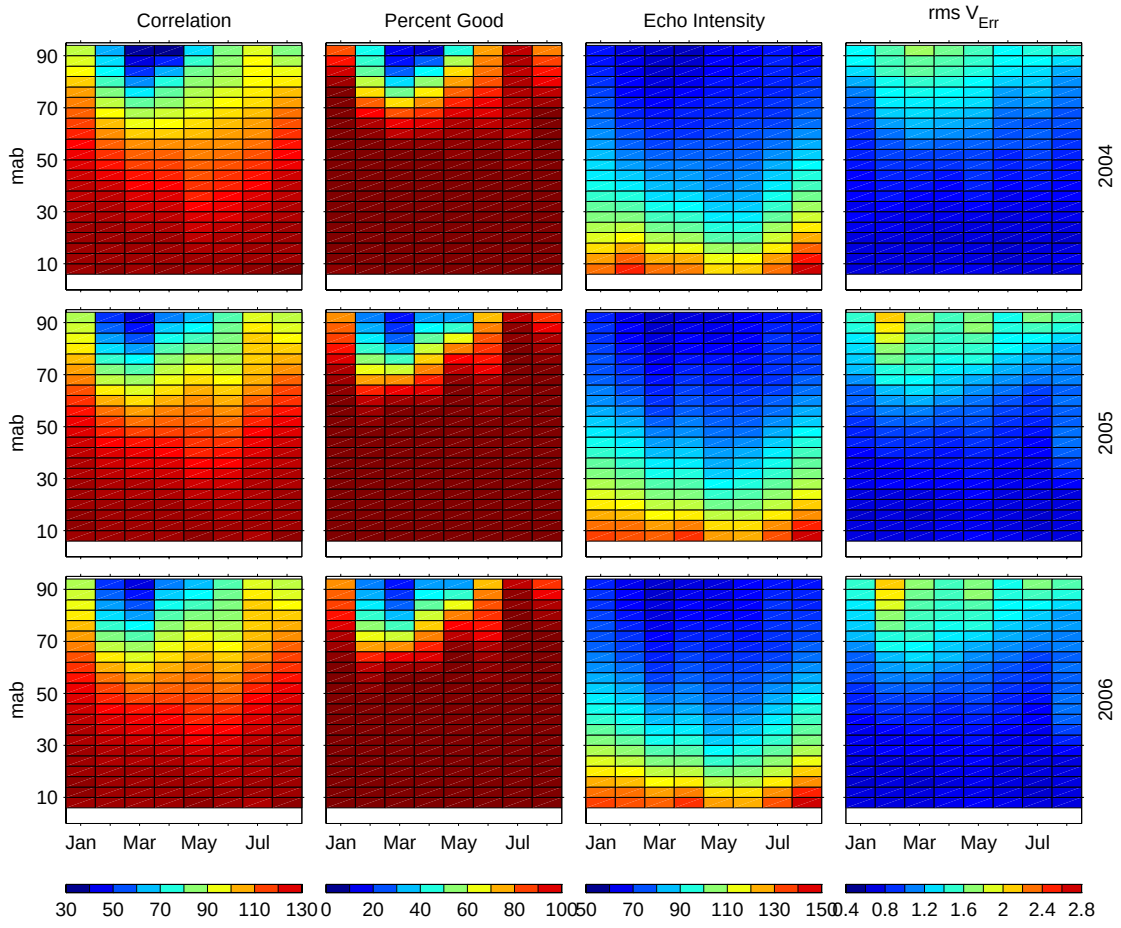

Figure 3. Monthly mean data quality parameters for (top row) 2004, (middle row) 2005 and (bottom row) 2006. Average correlation and echo intensity (over 4 beams) are in counts. Rms of error velocity is in cm/s. Percent good is the percentage of good data with 3 or 4 beam solutions.

Table 2. ADCP data quality statistics for each bin for years 2004-2006. The third column is the total percent of the flagged (bad) data. Error velocity, percent good and echo intensity are summarized with 5% and 95% quantiles, the mean and the standard deviation.

YEAR	Bin	Flagged (%)	Error velocity (cm s^{-1})				Percent Good (%)				Echo Intensity (counts)			
			5 %tile	95%tile	Mean	Std	5%tile	95%tile	Mean	Std	5%tile	95%tile	Mean	Std
2004	1	0	-1	1	0	0.62	96	100	99.46	1.51	111	152	128.84	12.48
	2	0	-1	1	0	0.61	96	100	99.64	1.28	106	147	123.81	12.41
	3	0.01	-1	1	-0.01	0.62	99	100	99.74	1.14	97	136	115.54	12.09
	4	0.03	-1	1	0	0.62	99	100	99.8	1.09	89	128	108.74	12.08
	5	0.04	-1.1	1.1	0	0.64	100	100	99.84	1.05	83	122	103.02	12.14
	6	0.05	-1.1	1.1	-0.01	0.67	100	100	99.88	1	79	117	98.17	12.17
	7	0.07	-1.1	1.1	0	0.69	100	100	99.9	0.93	75	113	93.88	12.11
	8	0.08	-1.2	1.2	0	0.72	100	100	99.9	0.9	72	110	90.31	11.99
	9	0.12	-1.2	1.2	0	0.73	100	100	99.89	1.03	70	107	87.04	11.94
	10	0.16	-1.2	1.2	0	0.76	100	100	99.86	1.13	68	105	84.13	11.91
	11	0.36	-1.3	1.3	0.01	0.79	99	100	99.79	1.45	66	102	81.23	11.7
	12	0.76	-1.3	1.3	0.01	0.83	99	100	99.67	1.88	64	99	78.55	11.3
	13	1.61	-1.4	1.4	0	0.88	99	100	99.5	2.32	63	96	76.03	10.64
	14	3.04	-1.5	1.5	0.01	0.93	96	100	99.21	3.03	62	93	73.89	10.04
	15	5.51	-1.6	1.6	0	0.99	93	100	98.9	3.65	62	90	72.12	9.49
	16	9.25	-1.7	1.7	-0.01	1.05	90	100	98.53	4.34	61	87	70.57	8.76
	17	14.4	-1.8	1.7	-0.02	1.1	87	100	98.13	4.87	61	85	69.41	8.06
	18	20.55	-1.9	1.9	0	1.17	84	100	97.8	5.22	60	83	68.51	7.54
	19	26.62	-2	2	-0.01	1.25	84	100	97.46	5.63	60	82	67.82	7.03
	20	33.14	-2.2	2.2	-0.01	1.32	81	100	97.24	5.84	60	81	67.3	6.65
	21	39.43	-2.4	2.3	-0.02	1.4	81	100	97.06	5.95	60	80	66.81	6.44
	22	45.69	-2.4	2.4	-0.02	1.47	81	100	96.66	6.3	60	80	66.36	6.32
	23	50.26	-2.7	2.6	-0.02	1.58	78	100	96	6.75	60	79	66.12	6.07
2005	1	0	-1	1.10	0.03	0.63	99	100	99.81	0.84	113	146	127.60	9.87
	2	0	-1	1	0.01	0.61	100	100	99.91	0.59	106	140	121.90	9.78
	3	0.01	-1	1	0.01	0.60	100	100	99.94	0.47	97	130	113.41	9.98
	4	0	-1	1	0	0.62	100	100	99.96	0.40	89	123	106.56	10.22
	5	0.01	-1	1	0.01	0.62	100	100	99.97	0.36	84	118	100.88	10.46
	6	0	-1.10	1.10	0.01	0.66	100	100	99.98	0.39	79	113	95.98	10.48
	7	0.01	-1.10	1.10	0.01	0.68	100	100	99.97	0.49	75	108	91.57	10.34
	8	0.02	-1.10	1.20	0.01	0.70	100	100	99.97	0.45	72	104	87.76	10.06
	9	0.04	-1.20	1.20	0.01	0.73	100	100	99.96	0.62	70	101	84.22	9.76
	10	0.08	-1.30	1.30	-0	0.77	100	100	99.93	0.69	68	98	81.04	9.41
	11	0.17	-1.30	1.30	-0.01	0.80	99	100	99.87	1.03	66	95	78.10	9.08
	12	0.44	-1.40	1.40	-0.01	0.85	99	100	99.73	1.66	64	92	75.36	8.54
	13	1.30	-1.50	1.40	-0.01	0.90	99	100	99.53	2.24	63	88	72.84	7.87
	14	3.03	-1.50	1.50	-0.01	0.95	96	100	99.15	3.14	62	84	70.76	7.37
	15	7.25	-1.60	1.60	-0.01	1.01	93	100	98.75	3.93	61	82	69.16	6.91
	16	13.20	-1.80	1.70	-0.01	1.10	90	100	98.38	4.46	61	80	67.94	6.40
	17	19.75	-1.90	1.90	-0.01	1.16	84	100	97.93	5.07	61	79	67.08	5.89
	18	26.75	-2	2	-0	1.25	84	100	97.54	5.44	60	77	66.41	5.50
	19	34.35	-2.10	2.10	-0.01	1.30	81	100	97.12	5.94	60	76	65.99	5.19
	20	41.78	-2.20	2.20	-0.02	1.35	81	100	96.98	6.04	60	75	65.66	4.82
	21	49.09	-2.40	2.30	-0.04	1.44	81	100	96.78	6.21	60	74	65.28	4.41
	22	56.01	-2.50	2.40	-0.04	1.49	78	100	96.45	6.48	60	73	64.90	4.18
	23	61.37	-2.80	2.80	-0.03	1.64	78	100	95.83	6.88	60	73	64.62	4.51
2006	1	0.01	-1	1.10	0.01	0.64	99	100	99.77	0.92	115	149	128.61	10.22
	2	0.02	-1	1	0.01	0.62	99	100	99.84	0.81	110	142	123.70	9.88
	3	0.02	-1	1	-0.01	0.63	99	100	99.88	0.69	100	132	115.31	9.72
	4	0.01	-1.10	1	-0.01	0.63	100	100	99.92	0.69	92	124	108.43	10.04
	5	0.07	-1.10	1.10	-0	0.65	100	100	99.93	0.76	85	118	102.71	10.33
	6	0.25	-1.10	1.10	-0.01	0.68	100	100	99.93	0.85	80	113	97.62	10.42
	7	0.49	-1.10	1.10	-0	0.70	100	100	99.92	0.96	76	109	92.92	10.42
	8	0.73	-1.20	1.20	-0.01	0.72	100	100	99.91	1.08	72	105	88.75	10.34
	9	0.98	-1.20	1.20	-0.01	0.75	100	100	99.89	1.19	69	102	84.84	10.23
	10	1.19	-1.30	1.20	-0.02	0.77	100	100	99.87	1.18	67	99	81.40	9.97
	11	1.40	-1.30	1.30	-0.02	0.81	99	100	99.81	1.31	65	96	78.19	9.59
	12	1.63	-1.40	1.40	-0.02	0.86	99	100	99.66	1.82	63	93	75.33	9.14
	13	2.28	-1.50	1.50	-0.03	0.91	96	100	99.38	2.59	62	90	72.85	8.69
	14	4.62	-1.60	1.60	-0.03	0.99	93	100	99	3.56	61	87	70.89	8.20
	15	8.25	-1.70	1.70	-0.04	1.06	93	100	98.71	4.05	61	85	69.33	7.74
	16	13.34	-1.90	1.80	-0.03	1.16	87	100	98.32	4.64	60	84	68	7.43
	17	19.72	-2.10	2.10	-0.03	1.28	84	100	97.93	5.18	60	82	66.97	7.03
	18	27.86	-2.40	2.30	-0.03	1.43	84	100	97.62	5.53	59	80	66.21	6.58
	19	36.84	-2.70	2.60	-0.04	1.55	84	100	97.52	5.53	59	78	65.80	6.07
	20	45	-2.90	2.80	-0.03	1.67	81	100	97.36	5.80	58	76	65.45	5.69
	21	52.65	-3	3	-0.02	1.75	81	100	97.42	5.82	59	76	65.18	5.40
	22	59.48	-3.30	3.20	-0.02	1.84	84	100	97.43	5.67	58	75	64.67	5.13
	23	65.76	-3.50	3.50	-0.05	1.99	81	100	97.27	5.86	58	74	64.30	4.75

5. ADCP Compass Correction

In contrast to the deployment in 2004, the concrete ballasts of the frames deployed in 2005 and 2006 comprised non-stainless-steel components. Owing to the large weight of the in situ bottom-mount and to the magnetic field of the vessel, we did not conduct compass calibration on board. In both years suspect to compass error, however, velocity profiles were collected close to the bottom-mounted (BM) ADCP by the vessel-mounted (VM) ADCP to aid possible correction of the BMADCP compass.

5.1. BMADCP – VMADCP Comparison: 2005

Four repeat occupations with VMADCP were made in the vicinity of the BMADCP:

11082005 1223-1231 UTC, 8x1-minute ensembles
11082005 1606-1620 UTC, 14x1-minute ensembles
11082005 1900-1910 UTC, 10x1-minute ensembles
11082005 2232-2240 UTC, 8x1-minute ensembles

North-East components of the velocity profiles measured by VMADCP are interpolated to height-above-bottom bins of the BMADCP and converted to speed and direction. The difference between the direction measured by VMADCP (Dir_{VM}) and BMADCP (Dir_{BM}) is calculated and unwrapped. Two anomalies delineated by Z-score value of $Dir_{VM} - Dir_{BM}$ exceeding twice the standard deviation are ignored before calculating the average value yielding the correction to the BM current direction. The histogram of $Dir_{VM} - Dir_{BM}$, the variability with respect to difference in speed, the outliers and the mean correction are shown in Figure 4. The scatter is significantly large and the BMADCP current direction cannot be expected to be accurate better than ±20° for year 2005.

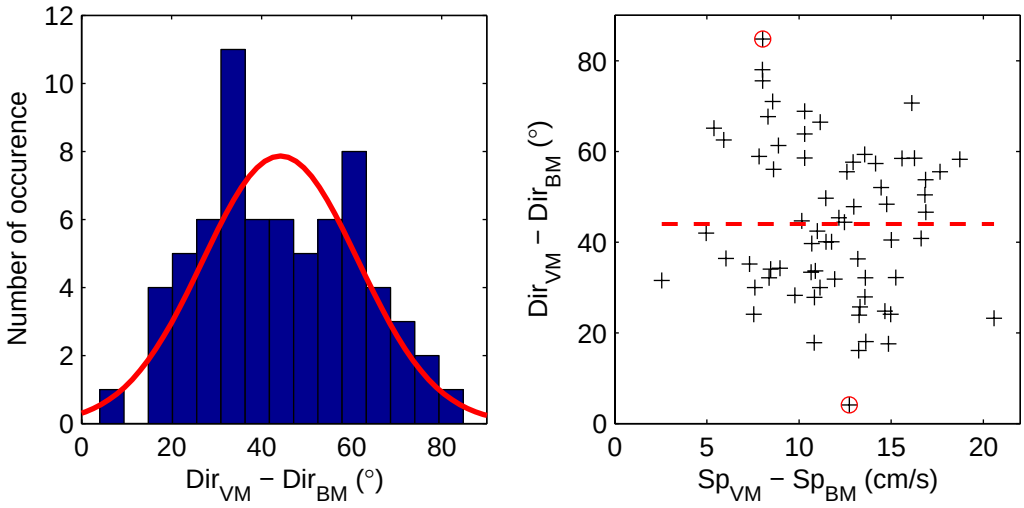

Figure 4. (Left) Histogram of the difference in current direction inferred from VMADCP (Dir_{VM}) and BMADCP (Dir_{BM}) together with a fit to the normal distribution. (Right) Scatter diagram of difference of VMADCP and BMADCP inferred direction and speed together with two outliers (red circles) and the mean correction of 44° (dashed red line).

Resulting speed and direction profiles averaged over each set of ensembles are shown in Figure 5. VMADCP does not resolve the near bottom layers. There is general agreement between the speed profiles, however comparison suggests that the accuracy of VMADCP measurements are questionable at low signal-to-noise ratio environment. The correction applied to BMADCP compass yields profiles consistent with those measured by VMADCP.

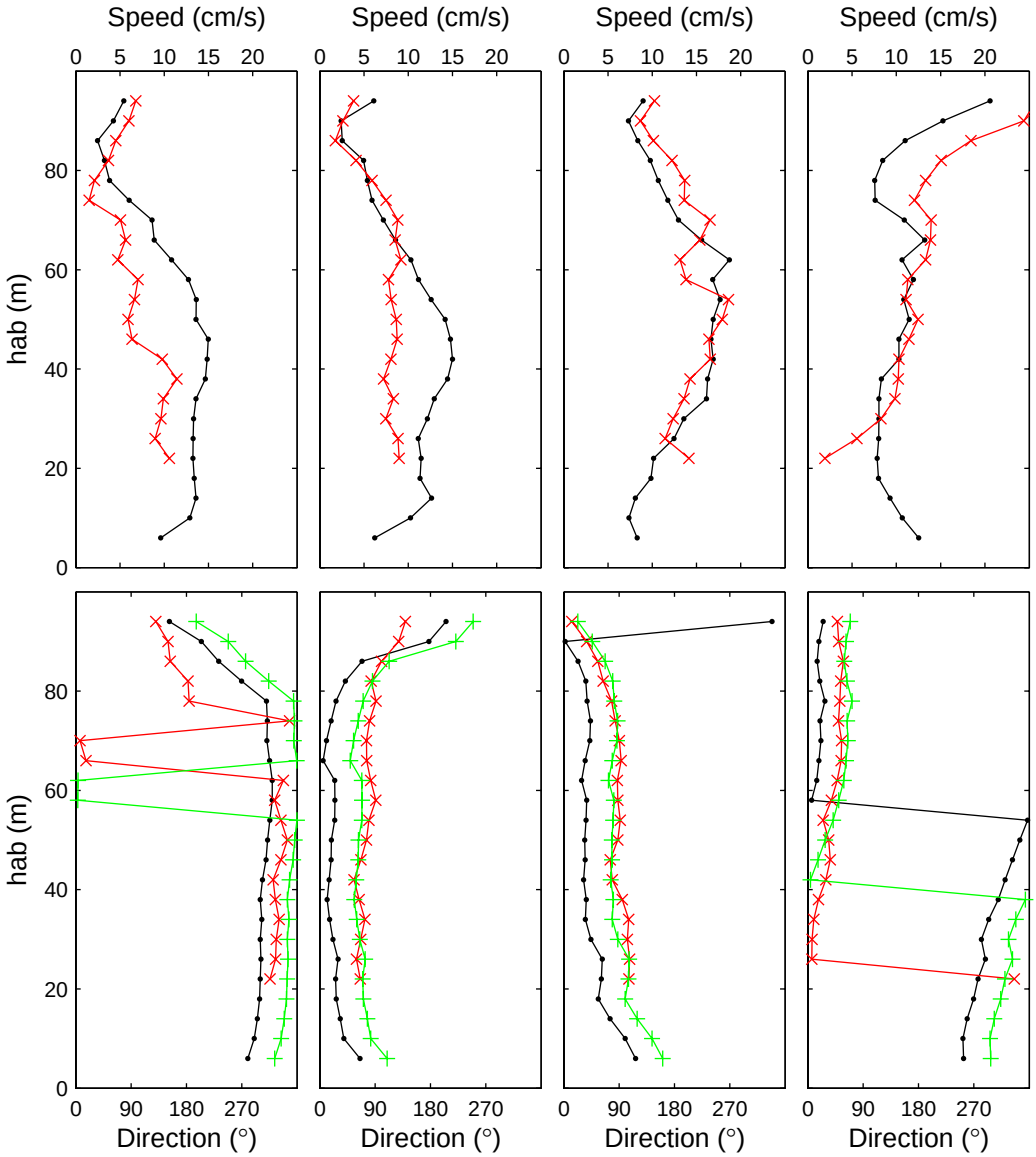

Figure 5. (Upper row) Profiles of current speed (red: VMADCP; black: BMADCP). (Lower row) Profiles of current direction (red: VMADCP; black: BMADCP; green: corrected BMADCP).

5.2. BMADCP – VMADCP Comparison: 2006

Before recovery of the ADCP on August 2006, the vessel switched off the thrusters and the engine to collect good quality ADCP data in the vicinity of the BMADCP. The last good 10-minute ensemble of BMADCP is on 09082006 1450 UTC until which 31 1-minute ensembles are available from the VMADCP. We vector-average the 1-minute ensembles derived from the VMADCP at 10 minute windows centered at the time of BMADCP 10-minute ensembles on 1430, 1440 and 1450 UTC. The speed and direction of the current for the three ensembles and their vector-average are shown in Figure 6. There is a discrepancy to within 5 cm/s in the speed profiles derived from BMADCP and VMADCP. Because the absolute current is not strong, the errors in the VMADCP derived current will be relatively significant due to corrections for the vessel motion. There is good agreement between the

direction derived from the instruments, and particularly below about 55 m, the agreement is excellent within the measurement uncertainty. The mean discrepancy in the direction of mean profiles from VMADCP and BMADCP is 24.8° between 34-94 m and reduces to 2.7° between 58-94 m. Note that for an ADCP mounted on a stable platform, the compass heading is accurate to within 5°. Upon this analysis, we conclude that no correction is necessary for the compass for the 2006 deployment.

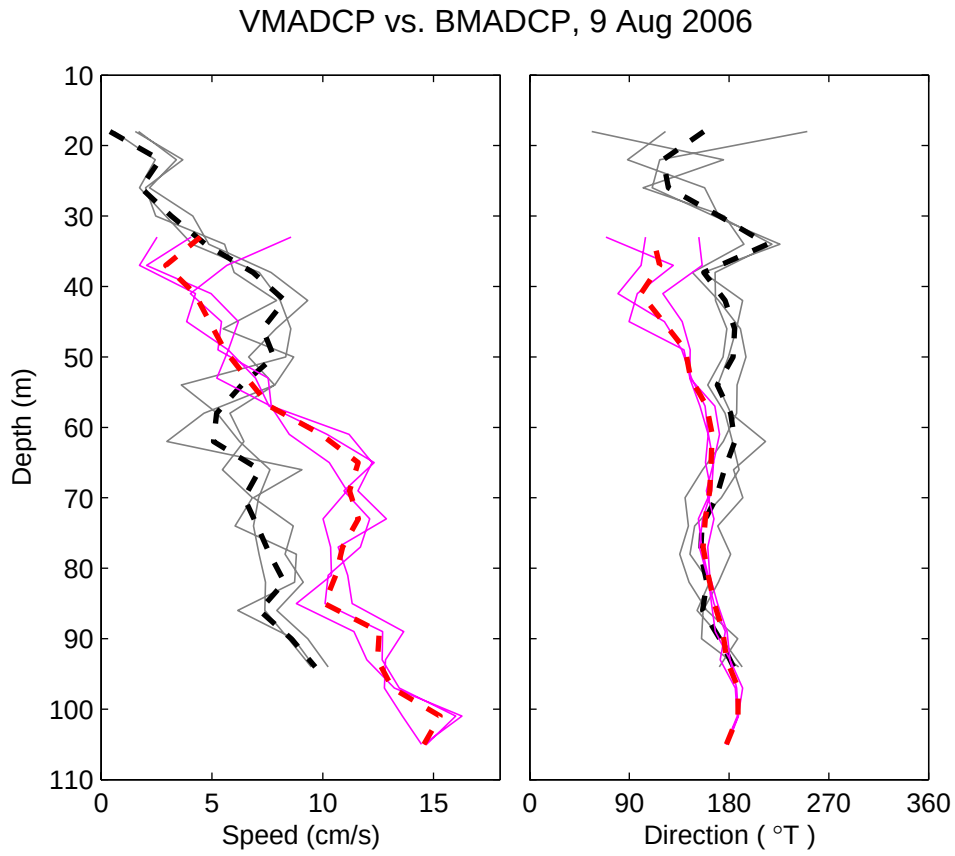

Figure 6. (Left) Speed and (right) direction profiles of the current inferred from 10-minute ensembles of BMADCP (magenta) on 9 August 2006 1430, 1440 and 1450 UTC and their mean (red dashed trace), three 10-minute ensembles of 1-minute VMADCP profiles (gray) centered at the time of BMADCP profiles and their mean (black, dashed trace) .

6. Microcat on the ADCP frame

SBE37-SM S/N 4011 (Microcat hereafter), calibrated on 30 August 2005 was deployed on the ADCP frame in 2006. The Microcat sampled and stored time, temperature, T, conductivity, C, and pressure, P, at 600 s intervals. Raw data set was spike free for all sensors. Salinity is calculated using 5-scan median filtered in situ T, C, and P and then despiked.

6.1. Correction of the Microcat Data

The Microcat installed on the frame of the 2006 deployment was not equipped with an internal pump for conductivity and was positioned horizontally. The conductivity record and salinity calculations therefore can be unreliable, especially so close to the bottom where the

conductivity cell can be contaminated by sediment and not flushed properly. We use two CTD profiles to check and correct the salinity derived from the Microcat.

On April 2006 several CTD stations were occupied from an ice floe close to the Storfjorden sill approached by Coast Guard KV Svalbard (data courtesy of R. Skogseth, UNIS). Field conditions did not allow for measurements at close proximity of the ADCP. The station closest to the ADCP was occupied on 23042006 0305 UTC, at 76° 59.95′ N, 019° 40.95′E approximately 10 km north-east of the mooring location at 117 m water depth. The second CTD profile was collected during the recovery cruise on 09082006 1412 UTC, at a position very close to the ADCP, right before the recovery.

Temperature-Salinity profiles and the Microcat record within ± 0.5 hour of each CTD profile are shown in Figure 7. Original salinity values derived from the Microcat are low and a constant offset of 0.41 is applied to match the CTD profiles. This correction might seem large, however, the data are then consistent with the two independent CTD profiles worked in different times of the deployment.

Temperature recorded by the Microcat is in excellent agreement with the CTD worked in April and is approximately 0.02K warmer in August. A correction to the Microcat temperature record was not deemed necessary.

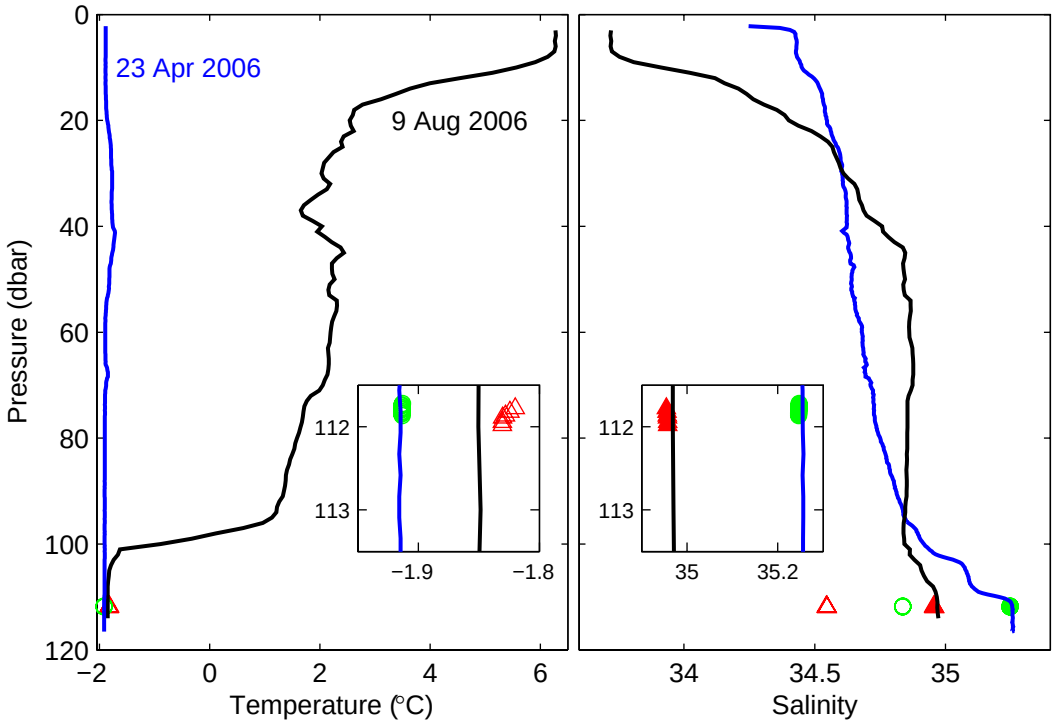

Figure 7. Comparison of SBE911+ system (left) temperature and (right) salinity profiles worked in (blue) 23 April 2006 and (black) 9 August 2006 with corresponding Microcat records within ± 0.5 h of the CTD deployment. Red and green markers correspond to April and August observations, respectively. While no correction was made to Microcat temperature records, filled markers for salinity indicate the correction (+0.41 offset) applied to the Microcat salinity data. Insets zoom into the parameter range of interest.

6.2. Microcat Data

Time series of temperature, salinity and pressure recorded by the Microcat is shown in Figure 8. A comparison of the ADCP – Microcat temperature sensors record shows that, on the average, ADCP records 0.05 K higher temperature (Figure 8a). No correction was

applied to the temperature sensors. Bottom temperature abruptly drops from about 1°C to zero on 5 March 2006 within 12 h. The decrease in temperature further continuous and the bottom temperature is less than -1.5 °C by 12 March. After April, near freezing point temperatures with S continuously in excess of 35 persist for about 2 months between 9 April and 10 June. Salinity gradually decreases for the rest of the record interrupted by typically 0.1 psu pulses of relatively higher salinity. Bottom pressure record shows predominantly tidal variations with major semidiurnal contribution and an apparent spring-neap cycle.

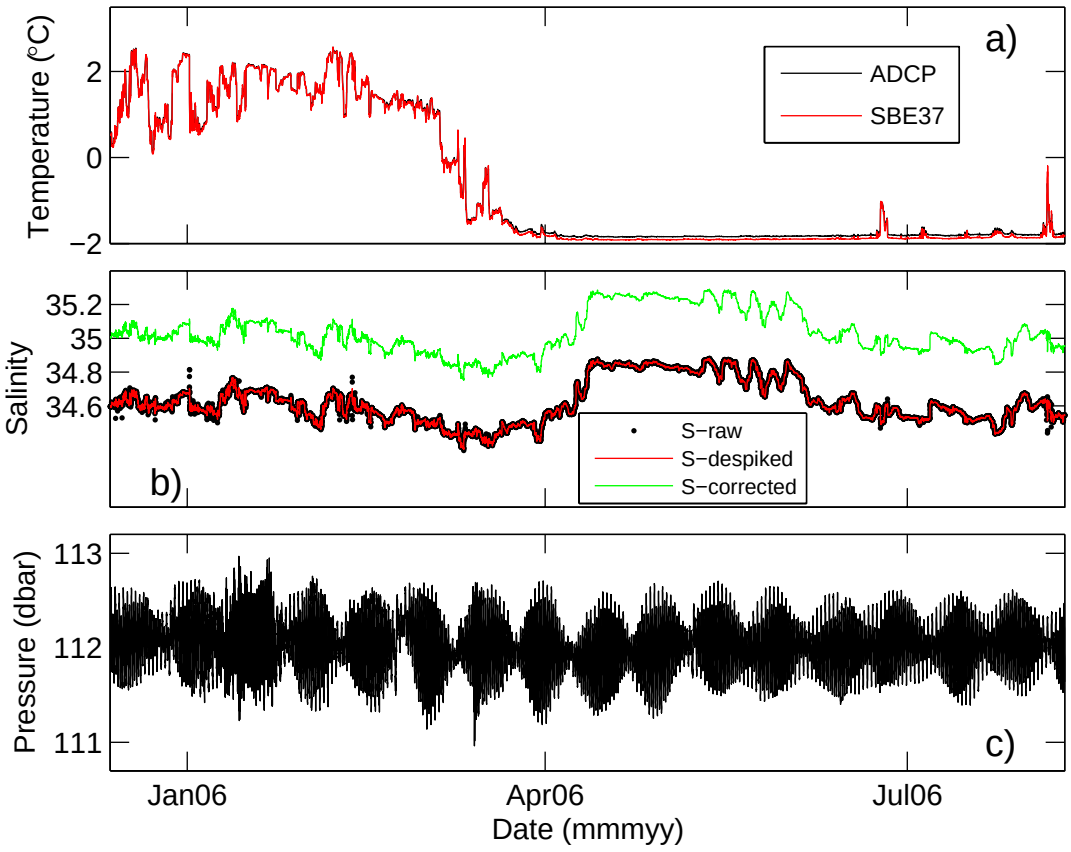

Figure 8. Time series of a) temperature b) salinity, and c) pressure recorded by the Microcat on the ADCP frame. Temperature record from the ADCP's temperature sensor is also shown in (a) (black trace). Salinity time series are the raw data points (black), the despiked values (red) and the final values obtained after correcting against CTD profiles (green).

The temperature-salinity diagram using daily averaged values further confirm the validity of the large salinity offset correction. In the early parts of the record, warm and saline water agree with the modified Atlantic Water characteristics of T > 0°C S > 34.8 at the site. There is isopycnal mixing along σ_θ = 28 ± 0.1 between T-S characteristics of East Spitsbergen Water (T from -1 to 0.5°C and S from 34.8 to 34.9). Later into the record temperature near freezing point is associated with brine enriched shelf water (with S>34.8).

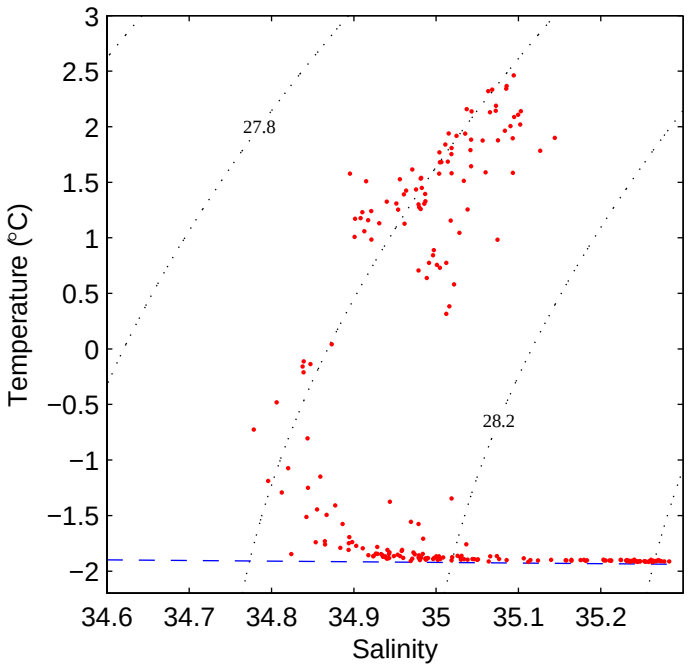

Figure 9. Temperature-Salinity diagram for daily averaged Microcat data. Isolines are σ_θ. Blue dashed line is the freezing point temperature for surface pressure.

Deterministic tidal frequencies show significant peaks in the frequency spectrum of the bottom pressure recorded by the Microcat (Figure 10). Noise dominates the record at frequencies above 0.3 cph. The dominant signal is semi-diurnal. Harmonic analysis of the pressure record resolves 59 constituents with signal-to-noise ratio greater than 2. The tidal prediction then accounts for 95% of the total variance. Some of the major constituents are given in Table 3. Lunar semi-diurnal tide dominates, and the total variance explained by the semidiurnal band alone (N_2+M_2+S_2) is 83.6%, consistent with the frequency spectrum. Most of the bottom pressure variance not explained by the tides is due to response to the atmospheric forcing, e.g. passage of strong wind events (Section 7).

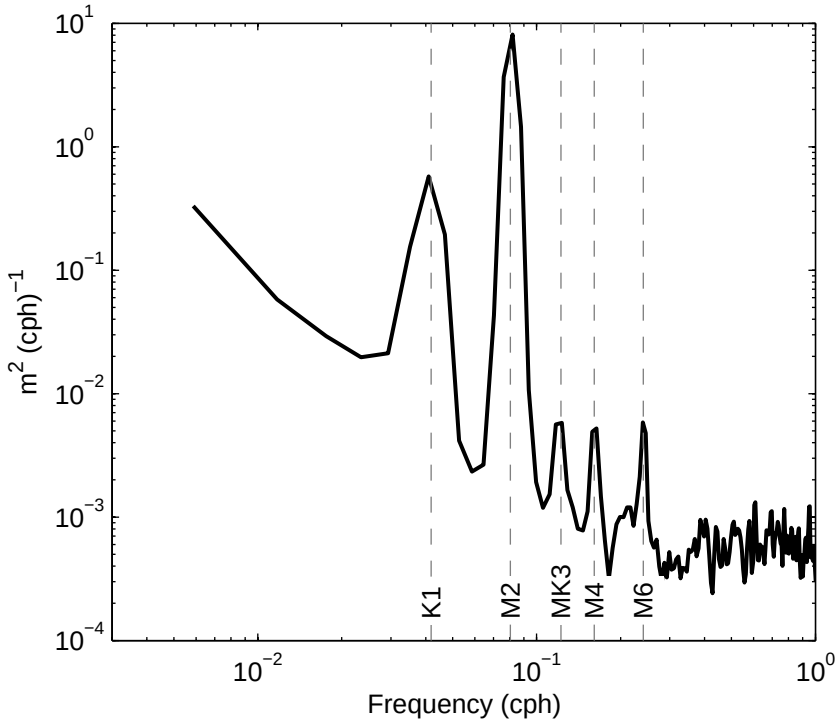

Figure 10. Frequency spectrum derived from the pressure recorded by the Microcat on the ADCP frame. Distinct tidal frequencies are indicated.

Table 3. Tides from the Microcat pressure sensor.

Constituent	Amplitudes (± CI) (m)	Phase (±CI) (°)	Variance Explained (%)
O_1	0.026 ± 0.004	39.4 ± 7.7	0.6
K_1	0.079 ± 0.003	331.5 ± 2.9	4.8
N_2	0.060 ± 0.003	277.1 ± 3.3	1.2
M_2	0.362 ± 0.004	301.0 ± 0.5	68.0
S_2	0.168 ± 0.003	357.9 ± 1.2	14.4
M_4	0.008 ± 0.001	68.4 ± 7.8	0.03

7. Atmospheric Forcing in 2006

Atmospheric data are available from the automated weather station in Edgeøya from July 2005 and on. Longer time series exist for stations at Bjørnøya, Hopen and Hornsund. However, because of its proximity to the Storfjorden polynya - which is the major drive for the overflow - Edgeøya is the most relevant meteorological station. Meteorological parameters are sampled every 6 hours and air temperature, wind speed and direction at 10 m height are presented in Figure 11 together with oceanic measurements at the sill. The data are 7-days low-passed. Following the winter months with air temperature reaching below -20°C, air temperature gradually increases after 1 April 2006, while the bottom water temperature at the sill is persistently near the freezing point. Between April and July, typical overflow months, air temperature varies between -5 – 2 °C with six cold events of 6 h duration (i.e., single data point) with temperature between -10 and -20 °C (not visible on low-passed presentation). These weather conditions after early April are not likely to cause significant freezing and brine formation. The wind direction after May 2006 seems suspiciously steady, suggesting instrument malfunction, however, raw data show variability between 0-15 °T with occasional pulses between 30-50 °T.

The bottom pressure record at the sill is de-tided and detrended to emphasize the response to atmospheric disturbances. Low frequency oscillations of typical ±0.1 dbar amplitude occur. The most significant peak, on 25 February is correlated with a strong wind event (and atmospheric pressure, not shown). Several other less significant peaks are similarly correlated to the atmospheric forcing. Lagged correlation analysis shows that bottom pressure anomaly is negatively correlated with the atmospheric pressure and the wind speed with zero time lag. The link between the cross-sill bottom current and atmospheric forcing, on the other hand, depends on the polynya activity and the time it takes for the newly generated BSW to feed the level of the sill. Lagged correlation between the wind speed and the bottom current at the sill shows a maximum at 2.5 days for both the 6-hourly sampled data and the low-passed data (Figure 12). Three such correlated wind-overflow events are marked by arrows in Figure 11. Strong wind, typically from NE consistent with the wind direction to maintain the polynya open, in winter leads to pulses of overflow directed out of the fjord.

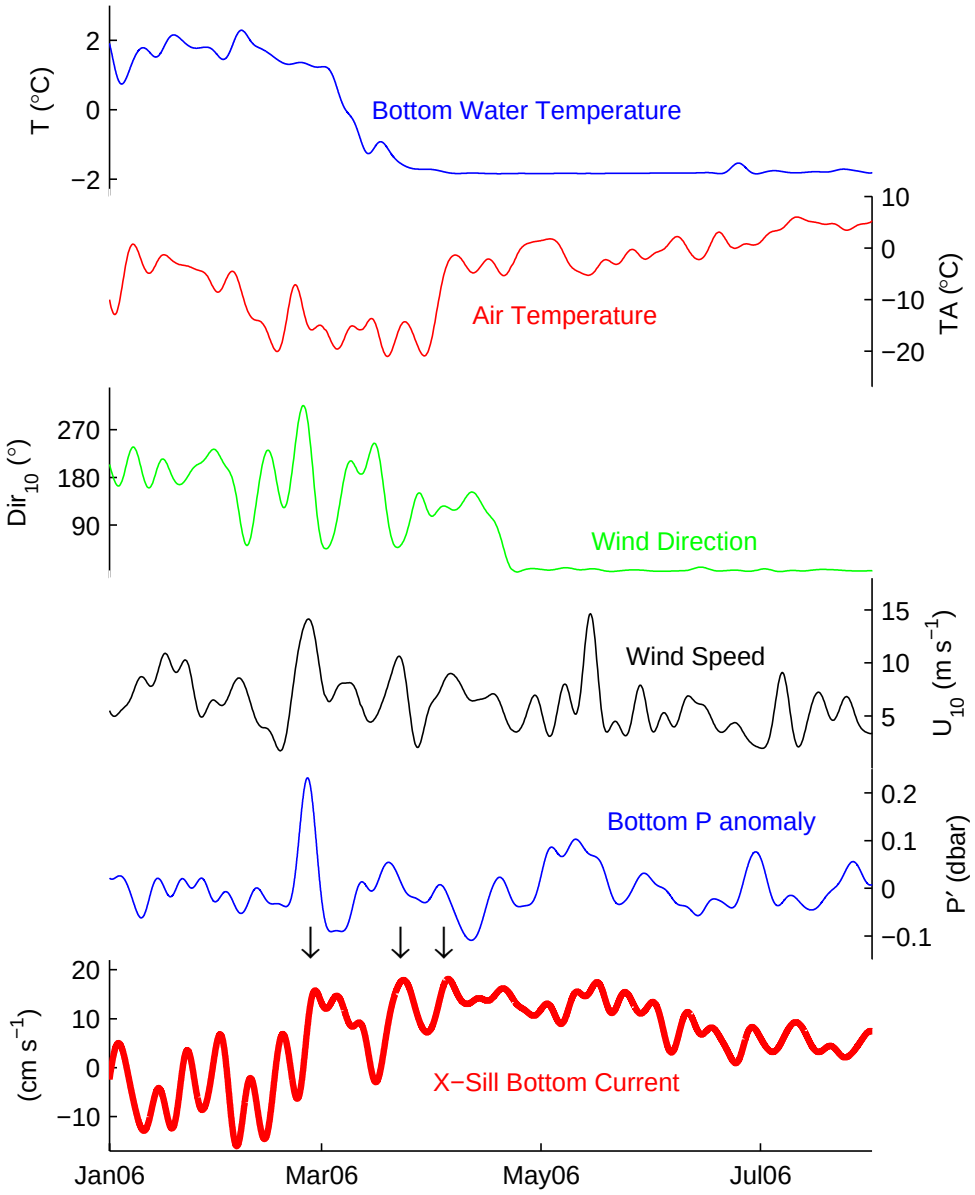

Figure 11. Seven-day low-pass filtered time series of bottom water temperature, air temperature, wind direction and speed at 10 m height, bottom pressure anomaly and cross-sill component of the bottom current. Bottom temperature and pressure anomaly is recorded by the Microcat. Cross-sill current is from the bottom-most bin of ADCP (6 mab). Bottom pressure anomaly is the detrended residual after tidal analysis. Meteorological data are sampled at Edgeøya at 6 hour intervals.

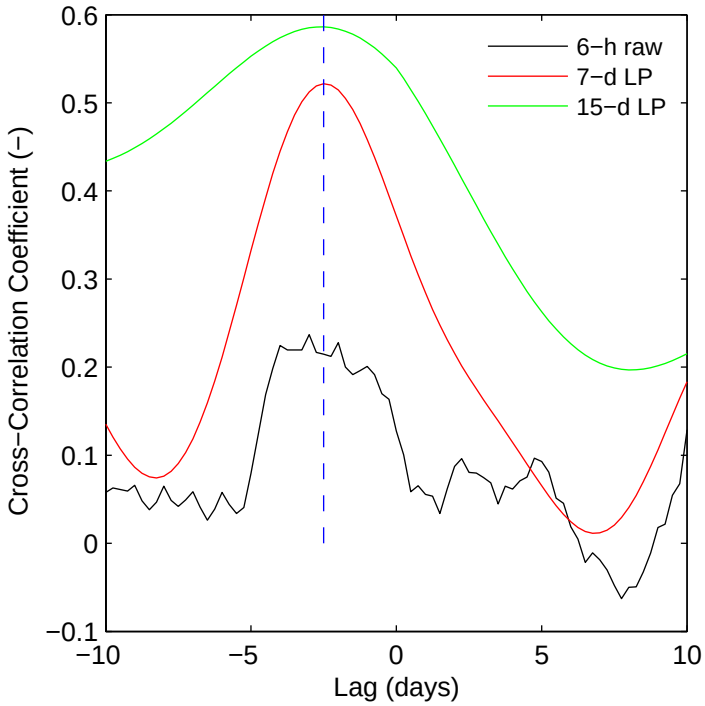

Figure 12. Lagged cross-correlation coefficient between cross-sill bottom current and wind speed measured at 10 m height at Edgeøya for the period in 2006 when the bottom temperature was less than 0 °C. Wind speed is sampled every 6 h. ADCP data is 6 hourly averaged to be consistent with the wind data. Vertical dashed line indicated the lag of maximum correlation at 2.5 days, wind at Edgeøya leading bottom current at the sill.

8. Current Data

Times series of current data from the three deployments are merged and presented in Figure 13 and Figure 14. Judging from the bottom temperature recorded by the ADCP, in 2005 the overflow reaches the sill about 2 months earlier than in 2004 and 2006 (Figure 13a). This is inferred as the first time of occurrence of bottom temperature of -1.8°C (1 April in 2004, 6 February in 2005 and 5 April in 2006). The transition from warm bottom temperatures to near freezing point significant increases from 2004 to 2006: The duration between the last time of occurrence of 0.5°C and the first time of appearance of -1.8°C is 60, 42 and 30 days, respectively for years 2004, 2005 and 2006. Interannual variability is also seen in the cross-sill component of the current (Figure 13b) and all three components of the velocity (Figure 14). In 2005, the east component of the velocity is comparable to the north component, in contrast to the other years. Note, however, the significant compass correction applied to year 2005 (Section 5.1).

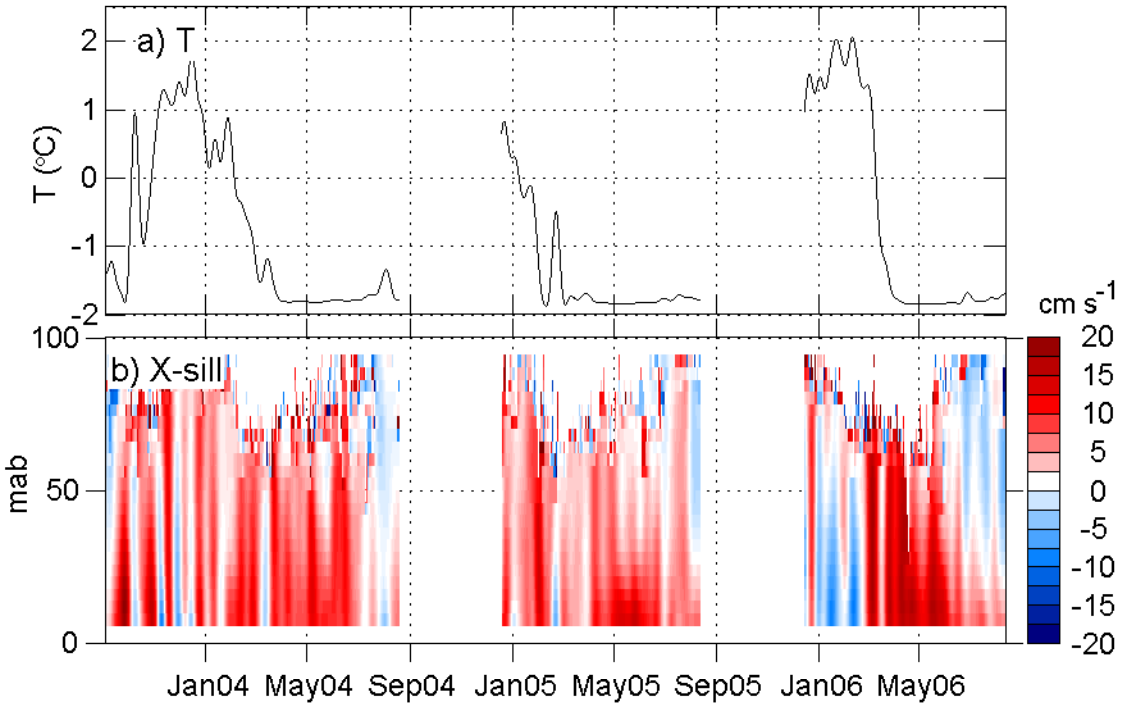

Figure 13. a) Bottom temperature record and b) cross-sill component of the velocity (positive values out of the fjord) for the period covering all three deployments. 15-day low-passed hourly data are presented. Noisy structure away from the bottom in b) is due to short segments of data which were not filtered.

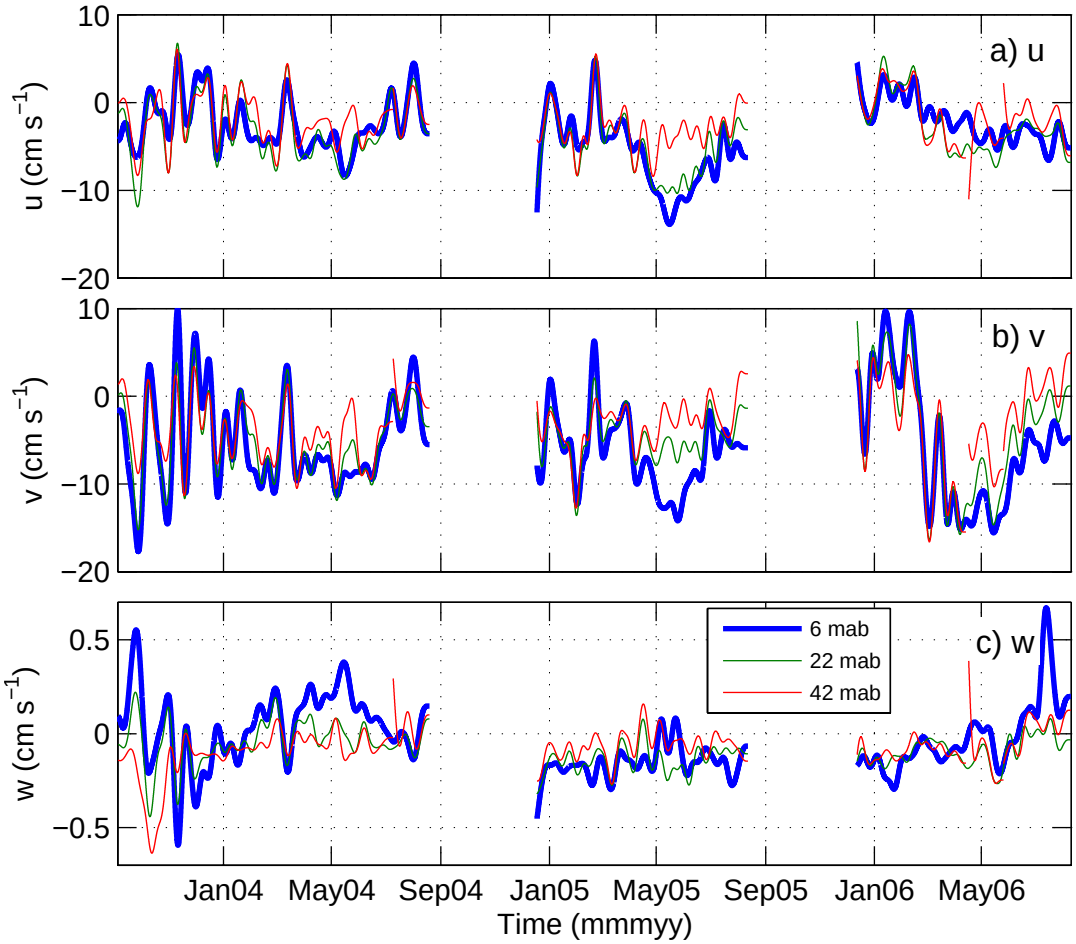

Figure 14. Time series of a) east b) north and c) vertical component of the velocity recorded by the ADCP at the sill. Record from three selected depths are shown: (blue) the bottommost cell 6 meter above bottom (mab), (green) 22 mab and (red) 42 mab. Data are hourly averaged and 15-day low-pass filtered. There are short gaps in the data from 42 mab owing to removed bad data. Anomalous velocity signal following a gap is an artifact of filtering.

Monthly mean current profiles are contrasted for each year in Figure 15. In January and February 2006, there is no signature of overflow at the sill: Bottom speed, on the average, is directed towards the fjord. For the corresponding months, there is a net out-fjord flow over the whole depth in years 2004 and 2005. In April and March, however, year 2006 has the strongest overflow, with speed approximately double that of the other years. The overflow persists in June 2004 throughout the water column, when the other years show weakened overflow in the bottom 40-50 m.

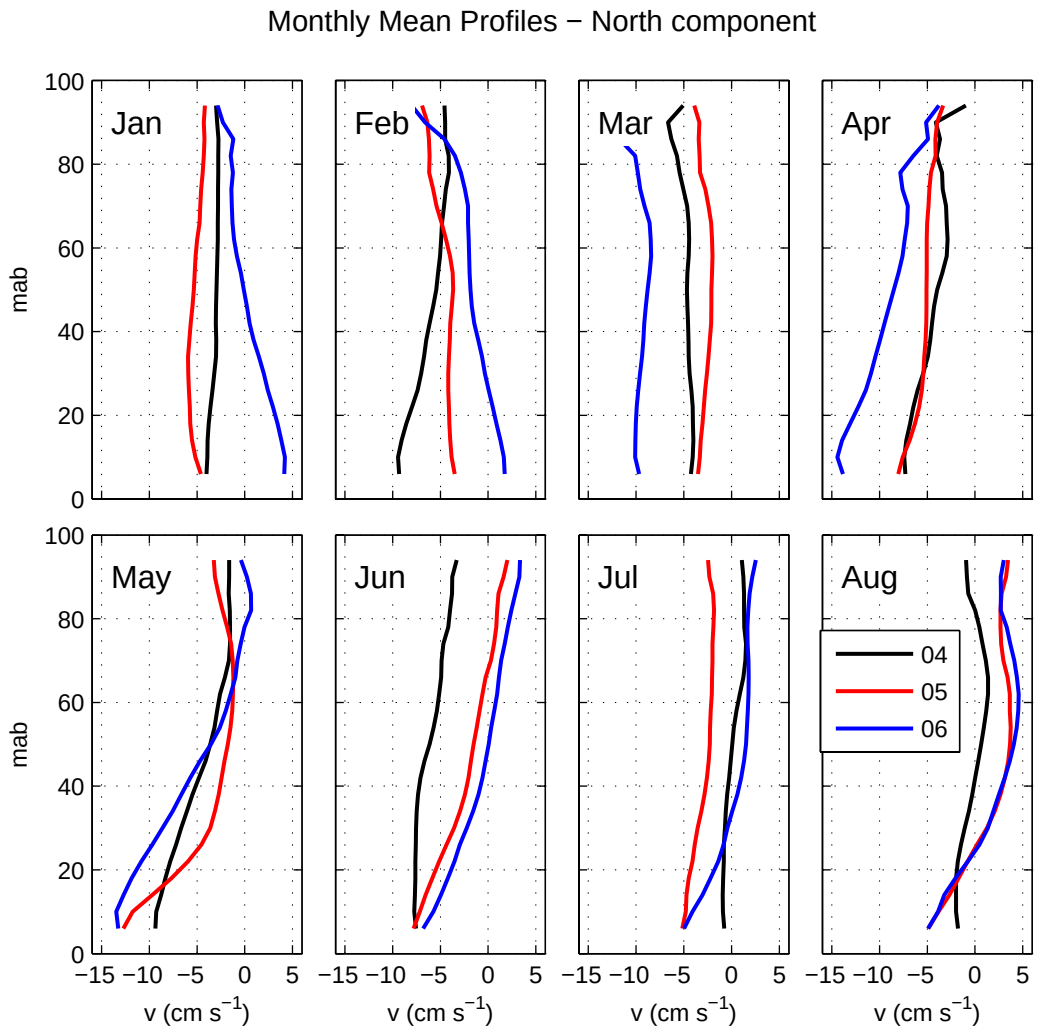

Figure 15. Monthly mean current profiles for the north component of the velocity shown for year (black) 2004, (red) 2005 and (blue) 2006. Negative values indicate approximately cross-sill flow directed out the fjord.

Progressive vector diagrams derived from low-passed currents show that northward cumulative displacement of the overflow is comparable for a common time frame (1 December – 30 June) for each year (Figure 16). On the other hand, there is significant variability in the zonal displacement. Year 2005 has the strongest westerly component of the flow.

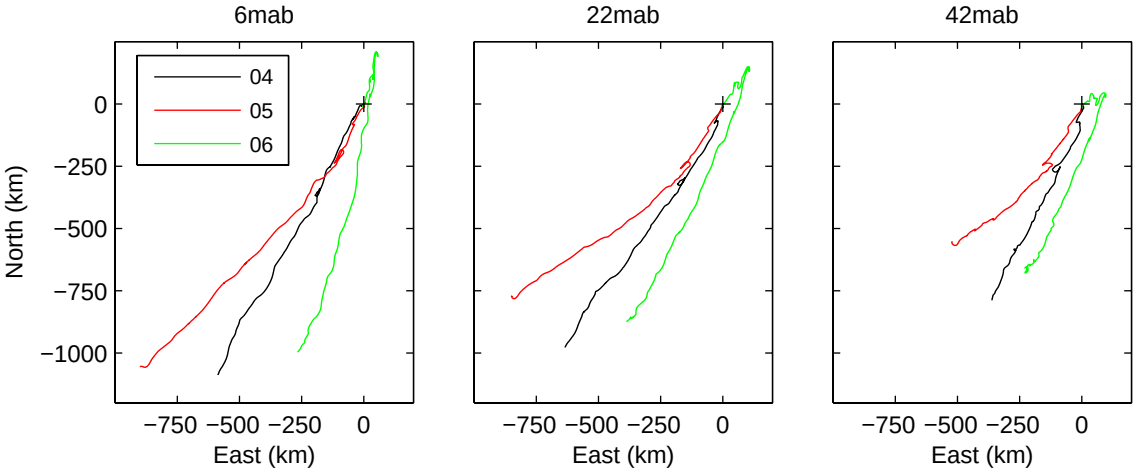

Figure 16. Progressive vector diagrams for the period 1 December to 30 June in (black) 2004, (red) 2005, and (green) 2006 derived from the bins 6, 22, and 42 m above bottom (mab). 15-day low-passed hourly data are shown.

9. Overflow Volume Transport

Overflow volume transport estimates are made assuming a sill width of B=15 km. This is chosen in order to be consistent with Schauer [1995] and the data report from year 2004[*Fer*, 2006]. The volume transport is Q = ⟨u⟩hB, where u is the plume speed (out of the fjord) and angle brackets denote averaging over the plume thickness, h. The plume speed is approximated with two alternatives: 1) The cross-sill component of the flow (approximately negative north component) and 2) any flow out of the fjord (i.e. directed within 90-270°T). Hourly averaged profiles are used. Overflow is assumed to occur when the bottom temperature is colder than -1.5°C and the near bottom u (averaged over the deepest 5 bins) is greater than 2 cm s^{-1}. The thickness of the plume is estimated as the height above bottom where u first falls below 2 cm s^{-1}. The transport is then calculated in Sverdrup (1 Sv = 10^6 m^3 s^{-1}) every hour. Weekly averages and standard deviation are shown in Figure 17 and Figure 18 for the transport normal to the sill and out of the fjord, respectively. The overflow is observed to occur 31%, 38% and 31% of years 2004, 2005, and 2006, respectively. The percentage given here is the ratio of the total hour of overflow record to total number of hours in one year (365x24). The overflow in 2005 starts relatively early. Among the years 2004 and 2006 with comparable duration of overflow, overflow in 2006 was marginally stronger on the average. In contrast to 2004, 2006 overflow was initially strong and significantly weakened after May.

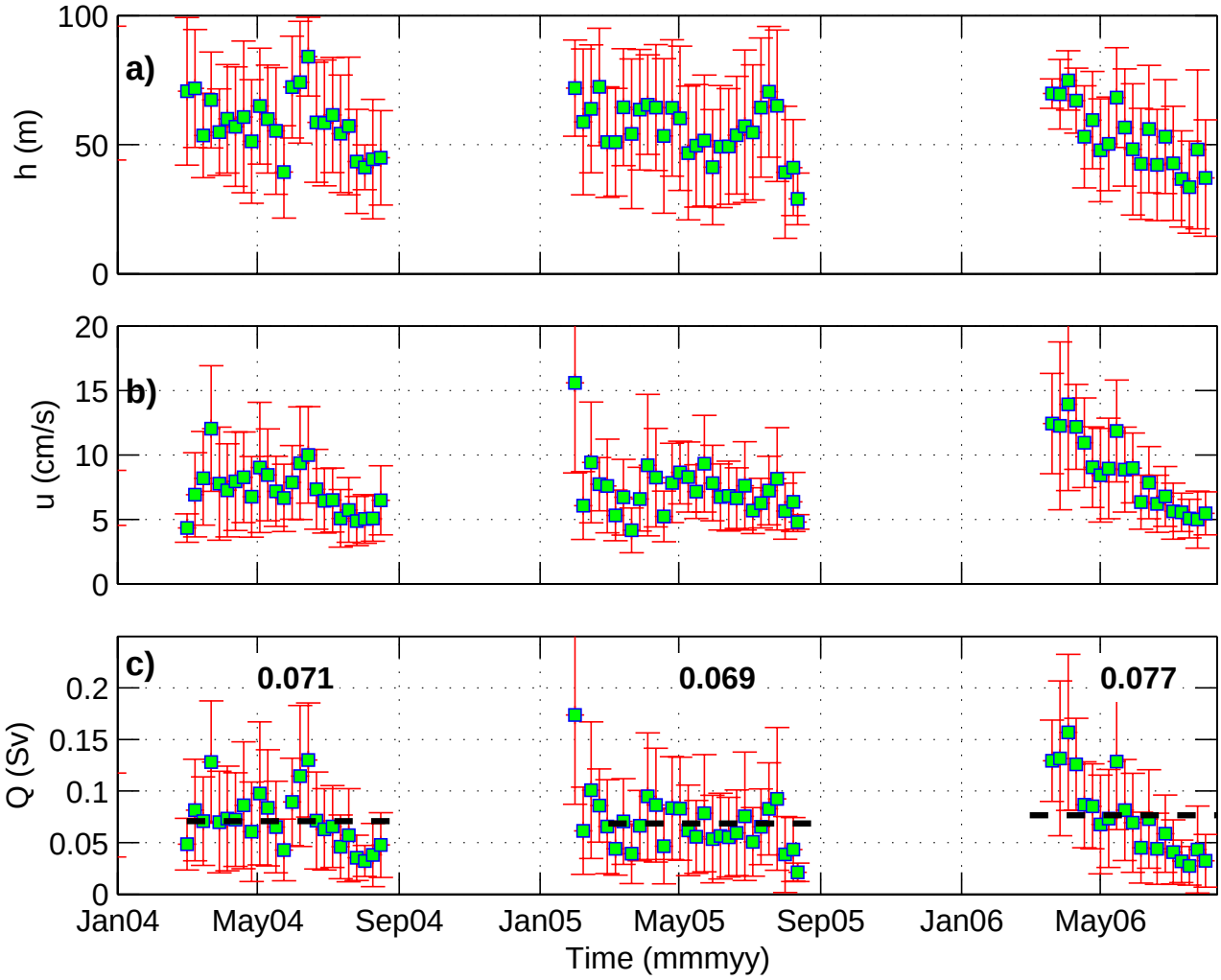

Figure 17. Weekly mean and standard deviation estimates for a) Storfjorden overflow plume thickness h, b) speed over the extend of h, and c) volume transport assuming a width of 15 km. Estimates are made using hourly averaged time series of cross-sill velocity profiles, using the following conditions: Near bottom speed (averaged over 5 deepest bins) must be greater than 2 cm/s and bottom temperature must be less than -1.5 °C. Plume thickness is the first bin above the bottom where the cross-sill velocity profile is less than 2 cm/s.

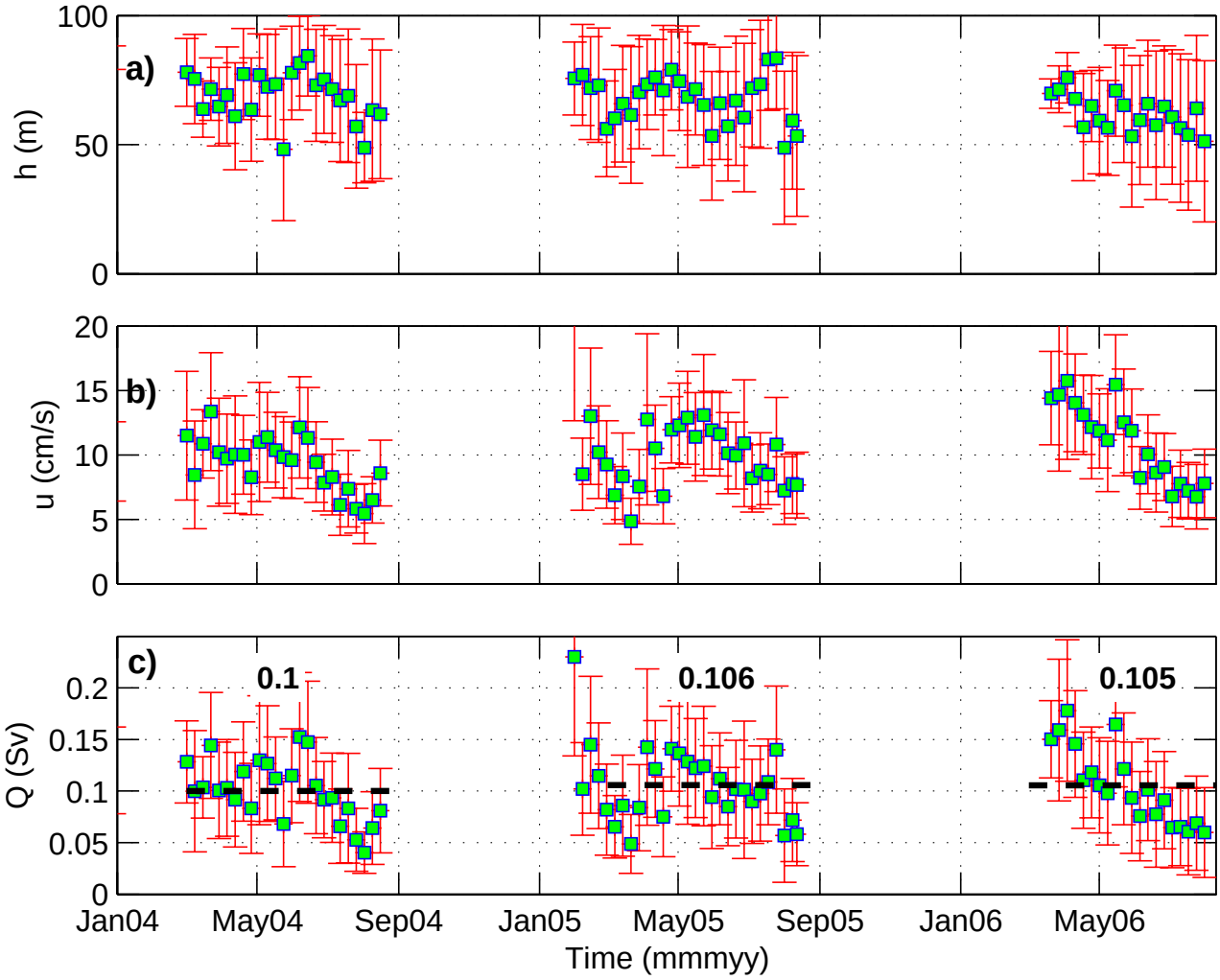

Figure 18. Same as Figure 17, but using data from the velocity profiles when the direction is between 90-270°T.

10. Concluding Remarks

Measurements were made of the current profiles at the Storfjorden sill for a total of 827 days between late 2003 and summer 2006. Data sampling was nearly continuous throughout the freezing period and was interrupted by several months in the fall. The bottom frame equipped with the 300 kHz ADCP and a Microcat is found to be efficient for monitoring the Storfjorden overflow. The volume transport estimates, however, will be uncertain owing to uncertainties in i) the guess on the width of the overflow plume and ii) the thickness of the plume. The overcome the latter, a kinematic threshold can be used to estimate the thickness of the plume. Further uncertainties arise due to the technical difficulties in calibrating the compass of the ADCP in situ. In this report we relied on the corrections inferred from accompanying ship-ADCP measurements. However, in Storfjorden where the mean current speed can be comparable to the corrections due to ship motions, inferred corrections can be inaccurate. A secondary complete system can help to overcome this problem. also serving as a back-up in case of instrument loss (i.e., while one system is in water, the second system can be calibrated and made deployment-ready in the lab.)

Data quality is found to be comparable for all years and the vertical range of good data varies seasonally between 70-90 m. The response to atmospheric forcing is seen in the near-bottom current measurements. Two modes of response to the atmospheric forcing is likely: i) the polynya will response to cold/windy events and newly produced dense waters will lead to pulses at the sill after a time lag (inferred 2.5 days lag in 2006) ii) passage of local low-pressure system has signature on the bottom pressure and current record.

Initiation of the overflow and overflow duration, inferred from cold bottom temperature period and the velocity structure at the sill are found to vary interannually. Strongest overflows are between April and May with bottom speeds reaching 15 cm/s. Albeit the interannual variability in the thickness of the plume, the current structure and the duration, estimates of volume transport are found to be fairly constant for each year. The lower and upper bounds on the mean transports (averaged over overflow duration) are estimated to be 0.07 and 0.11 Sv.

APPENDIX A: Configuration of Sentinel ADCP

Below is the configuration files, identical for deployments in 2004, 2005 and 2006, except for the “Time of first ping” TF03/09/04 12:00:00 for 2004, TF17/12/04 00:00:00 for 2005 and TF12/12/05 00:00:00 for 2006.

CR1	*Parameters set to factory defaults*
CF11101	*Flow control*
EA0	*Heading alignment*
EB0	*Heading bias*
ED0	*Transducer depth*
ES35	*Salinity*
EX11111	*Coordinate transformation*
EZ1111111	*Sensor source*
WB0	*Bandwidth control*
WD1111000000	*Data out*
WF176	*Blank after transmission*
WN30	*Number of depth cells*
WP33	*Pings per ensemble*
WS400	*Depth cell size*
WV170	*Ambiguity velocity*
TE00:10:00.00	*Time per ensemble*
TF…..	*Time of first ping*
TP00:18.18	*Time between pings*
CK	*Parameters save as USER defaults*
CS	*START*

;
;Instrument = Workhorse Sentinel
;Frequency = 307200
;Beam angle = 20
;Temperature = 5.00
;Deployment hours = 7200.00
;Battery packs = 2
;Automatic TP = YES
; Memory size [MB] = 256

;Consequences generated by PlanADCP version 2.01:
;First cell range = 5.96 m
;Last cell range = 121.96 m
;Max range = 111.53 m
;Standard deviation = 0.54 cm/s
;Ensemble size = 748 bytes
;Storage required = 32.31 MB
;Power usage = 669.32 Wh
;Battery usage 1.5

References

Fer, I. (2006), Current Measurements at the Storfjorden Sill 76° 58′N, 19° 15′E, September 2003 – August 2004, University of Bergen, ISBN 82-8116-007-1. 41s., Bergen.

Fer, I., R. Skogseth, and P. M. Haugan (2004), Mixing of the Storfjorden overflow (Svalbard Archipelago) inferred from density overturns, *J. Geophys. Res.*, *109*, C01005, doi:10.1029/2003JC001968.

Fer, I., R. Skogseth, P. M. Haugan, and P. Jaccard (2003), Observations of the Storfjorden overflow, *Deep-Sea Res. I*, *50*, 1283-1303.

Quadfasel, D., B. Rudels, and K. Kurz (1988), Outflow of dense water from a Svalbard fjord into the Fram Strait, *Deep-Sea Res.*, *35*, 1143-1150.

RDI (1996), Acoustic Doppler Current Profiler. Principals of Operation. A practical Primer., San Diego, California, USA.

Schauer, U. (1995), The release of brine-enriched shelf water from Storfjord into the Norwegian Sea, *J. Geophys. Res.*, *100*, 16,015-16,028.

Schauer, U., and E. Fahrbach (1999), A dense bottom water plume in the western Barents Sea: downstream modification and interannual variability, *Deep-Sea Res.*, *46*, 2095-2108.

Skogseth, R., I. Fer, and P. M. Haugan (2005a), Dense-water production and overflow from an Arctic coastal polynya in Storfjorden, in *The Nordic Seas: An Integrated Perspective*, edited by H. Drange, et al., pp. 73-88, AGU Geophysical Monograph, 158.

Skogseth, R., P. M. Haugan, and M. Jakobsson (2005b), Water mass transformations in Storfjorden, *Cont. Shelf Res.*, *25*, 667-695.